Electronic Supplementary Material (ESI) for Sustainable Energy & Fuels.

Bipyrimidine Core Structure-based Hole Transport Material for Efficient Perovskite Solar Cells

Yang Yang[a], Fei Wu,*[a] Huiqiang Lu[a], Shufang Li[a], Cheng Zhong[b]*,Linna Zhu*[a]

[a]*Chongqing Key Laboratory for Advanced Materials and Technologies of Clean Energy, School of Materials & Energy, Southwest University, Chongqing 400715, P.R. China.*

[b]*Hubei Key Lab on Organic and Polymeric Optoelectronic Materials, Department of Chemistry, Wuhan University. Wuhan 430072, P. R. China.*

Corresponding Author: *Linna Zhu, School of Materials & Energy, Southwest University, Chongqing, China, E-mail address: lnzhu@swu.edu.cn. Tel.: +86 23 68254957.*

Fei Wu, School of Materials & Energy, Southwest University, Chongqing, China, E-mail address: feiwu610@swu.edu.cn.

Table of contents

1. General information

Unless otherwise stated, all starting materials were purchased from commercial suppliers (Sigma Aldrich, and the Energy Chemical) and used without further purification. The nuclear magnetic resonance (NMR) spectra were obtained from a BRUKER AVANCE Ⅲ 600 MHz NMR Instrument (in $CDCl_3$). MALDI-TOF HRMS was performed on a Bruker Autoflex instrument, using 1,8,9-trihydroxyanthracene as a matrix. UV-vis absorption spectra were measured on a Shimadzu UV-2450 absorption spectrophotometer. Cyclic voltammetry (CV) test was performed on a CHI-660A in $CDCl_3$ under a nitrogen atmosphere, using a saturated calomel electrode (SCE) as a reference electrode and ferrocene as an internal standard. Thermal gravimetric analysis (TGA) was performed on a TGA Q50 at a heating rate of 10 °C min^{-1} under a nitrogen atmosphere. Differential scanning calorimetry (DSC) measurement was performed on a DSC Q20 instrument at a heating rate of 10 °C min^{-1} under a nitrogen atmosphere. The cross-sectional SEM image of the device was characterized by FE-SEM images (JSM-7800F). Atomic force microscopy (AFM) was used for characterizing the morphology using a CSPM5500. Water contact angles were measured on contact angle measurement apparatus JC2000D, Shanghai Zhongchen Digital Technology Co., Ltd., China. Steady-state PL spectra were recorded on Fluorolog®-3 fluorescence spectrometer (Horiba). Time-resolved PL decay curves were measured by a single photon counting spectrometer from Horiba Instruments (Fluorolog®-3) with a Picosecond Pulsed UV-LASTER (LASTER375) as the excitation source. The current–voltage (*J–V*) curves were measured under 100 mW cm^{-2} (AM 1.5 G) simulated sunlight using Keithley 2400 in conjunction with a Newport solar simulator (94043A). The external quantum efficiency (EQE) was calculated from the photocurrent measurement under monochromatic illuminations at different wavelengths, using a 150 W xenon lamp and a monochromator.

2. Synthetic procedures and characterization

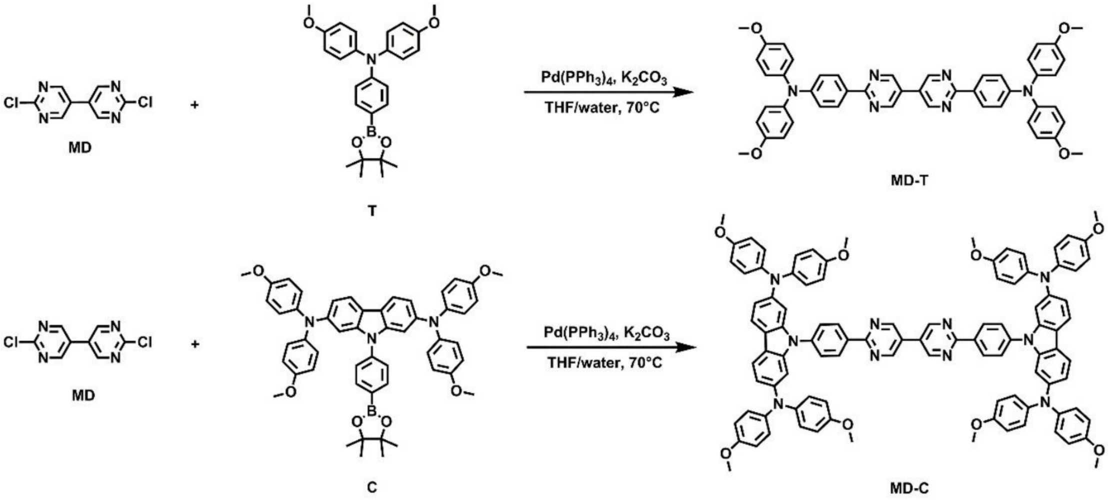

Scheme S1. The synthesis route of **MD-T and MD-C**

The intermediate **MD** and **Compound T** and **C** synthesized according to the method reported in the literature[1, 2].

Synthesis of *MD-T* (4'-([5, 5'-bipyrimidine]-2, 2'-diyl)bis(N,N-bis(4-methoxyphenyl) aniline))

Compound **T** (427 mg, 0.99mmol), MD (90mg, 0.39mmol), Pd (PPh$_3$)$_4$ (34.6 mg, 0.03 mmol), K$_2$CO$_3$ solution (1.5 mL, 2 M in H$_2$O) were dissolved in distilled THF (30 mL). The reaction mixture was heated to 70 °C with stirring overnight. Then the mixture was cooling down to room temperature. The mixture was extracted with dichloromethane and washed several times with brine. The organic layer was dried with anhydrous magnesium sulfate. The filtrate was then evaporated under vacuum and purified by column chromatography (methyl alcohol / dichloromethane =1/20) to give **MD-T** as a yellow solid (181.8 mg, 60%); ^{1}H NMR (600 MHz, CDCl$_3$) δ 8.96 (s, 4H), 8.27 (d, J = 8.8 Hz, 4H), 7.13 (d, J = 8.8 Hz, 8H), 6.97 (d, J = 8.9 Hz, 4H), 6.87 (d, J = 8.9 Hz, 8H), 3.82 (s, 12H). ^{13}C NMR (151 MHz, CDCl$_3$) δ 164.33, 156.60, 154.42, 151.52, 140.02, 129.33, 127.94, 127.46, 124.75, 118.68, 114.88, 55.50. HRMS m/z: [M+H]$^+$ calcd for 765.3111; found 765.3184.

Synthesis of *MD-C* (9,9'-([5,5'-bipyrimidine]-2,2'-diylbis(4,1-phenylene))bis(N2,N2,N7,N7-tetrakis(4-methoxyphenyl)-9H-carbazole-2,7-diamine))

Compound **C** (271.8mg, 0.33mmol), MD (30mg, 0.13mmol), $Pd(PPh_3)_4$ (11.55 mg, 0.01 mmol), K_2CO_3 solution (0.5 mL, 2 M in H_2O) were dissolved in distilled THF (20 mL). The reaction mixture was heated to 70 °C with stirring overnight. Then the mixture was cooling down to room temperature. The mixture was extracted with dichloromethane and washed several times with brine. The organic layer was dried with anhydrous magnesium sulfate. The filtrate was then evaporated under vacuum and purified by column chromatography (methyl alcohol / dichloromethane =1/20) to give **MD-C** as a saffron yellow solid (114.5 mg, 56%) ^{1}H NMR (600 MHz, THF) δ 9.12 (s, 4H), 8.51 (d, *J* = 8.5 Hz, 4H), 7.70 (d, *J* = 8.4 Hz, 4H), 7.43 (d, *J* = 8.5 Hz, 4H), 6.99 (s, 4H), 6.88 (d, *J* = 7.3 Hz, 16H), 6.74 (s, 4H), 6.67 (d, *J* = 8.7 Hz, 16H), 3.61 (s, 24H). ^{13}C NMR (151 MHz, $CDCl_3$) δ^{13}C NMR (151 MHz, $CDCl_3$) δ 163.92, 154.85, 141.83, 140.46, 135.01, 132.15, 132.08, 131.95, 129.84, 128.56, 128.48, 126.29, 125.87, 114.56, 103.94, 55.23.

MALDI-TOF m/z: $[M+H]^+$ calcd for $C_{100}H_{80}N_{10}O_8$: Cal 1549.4595; found 1549.6239.

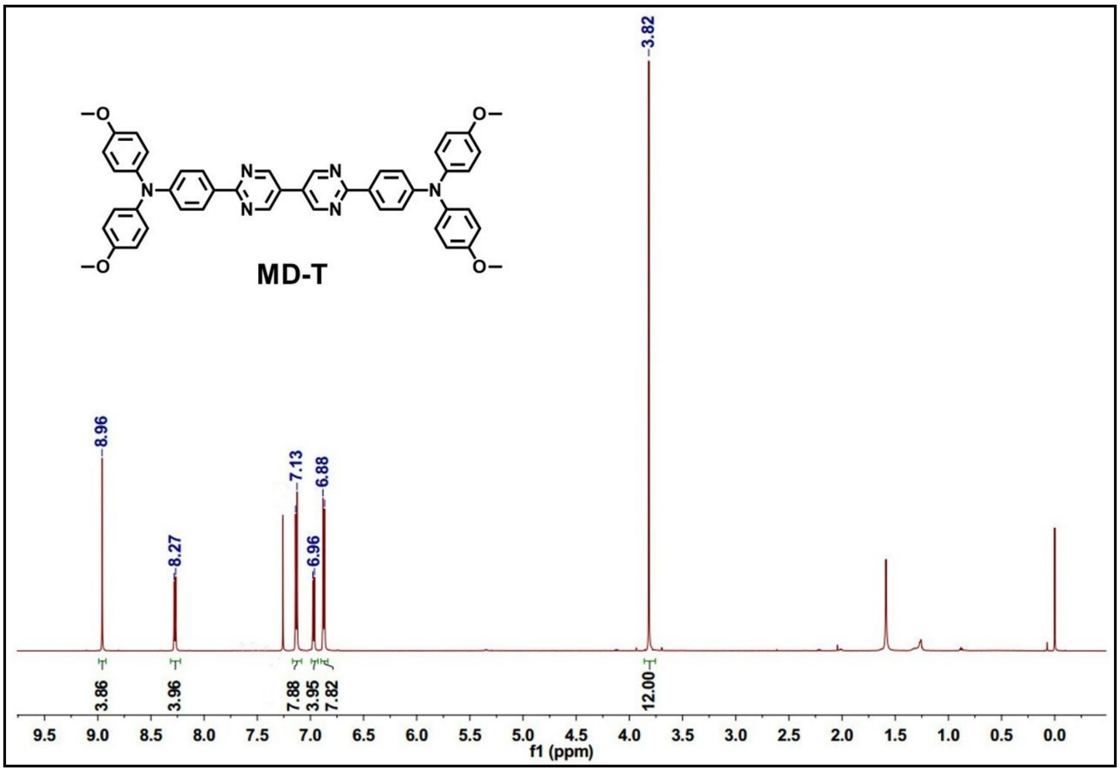

Figure S1. ^{1}H NMR spectrum of **MD-T** in $CDCl_3$.

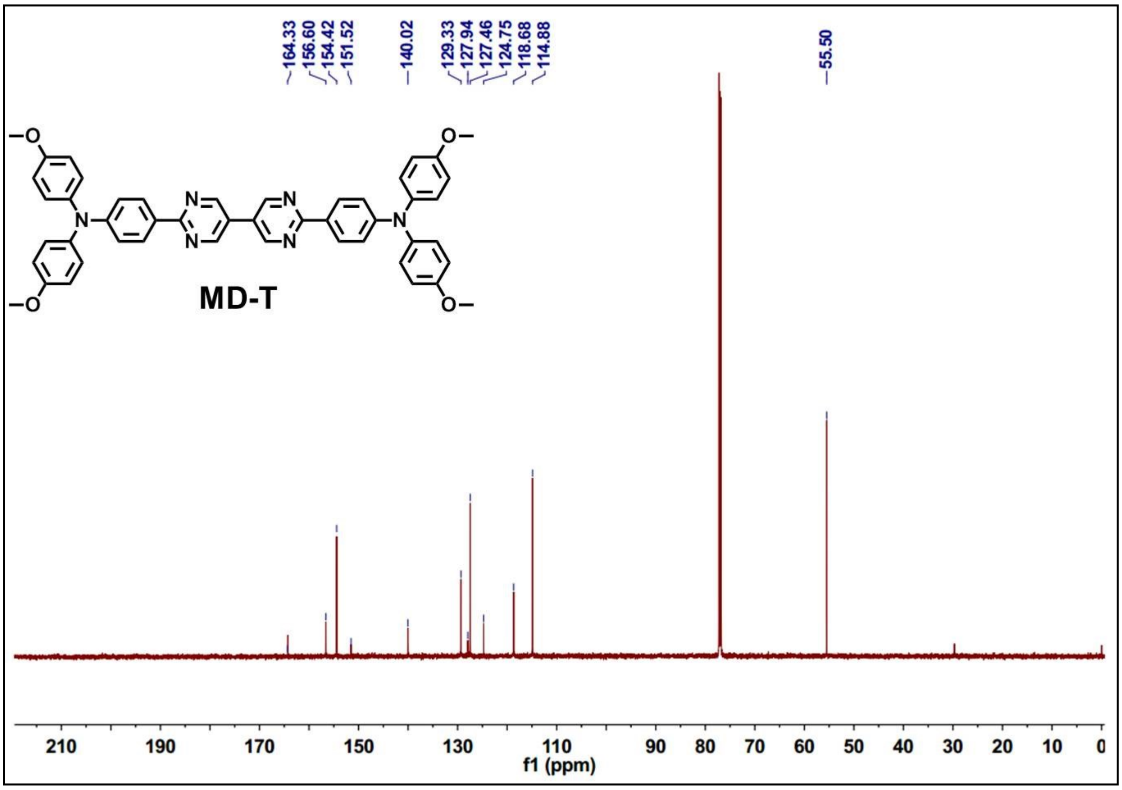

Figure S2. ^{13}C NMR spectrum of **MD-T** in $CDCl_3$.

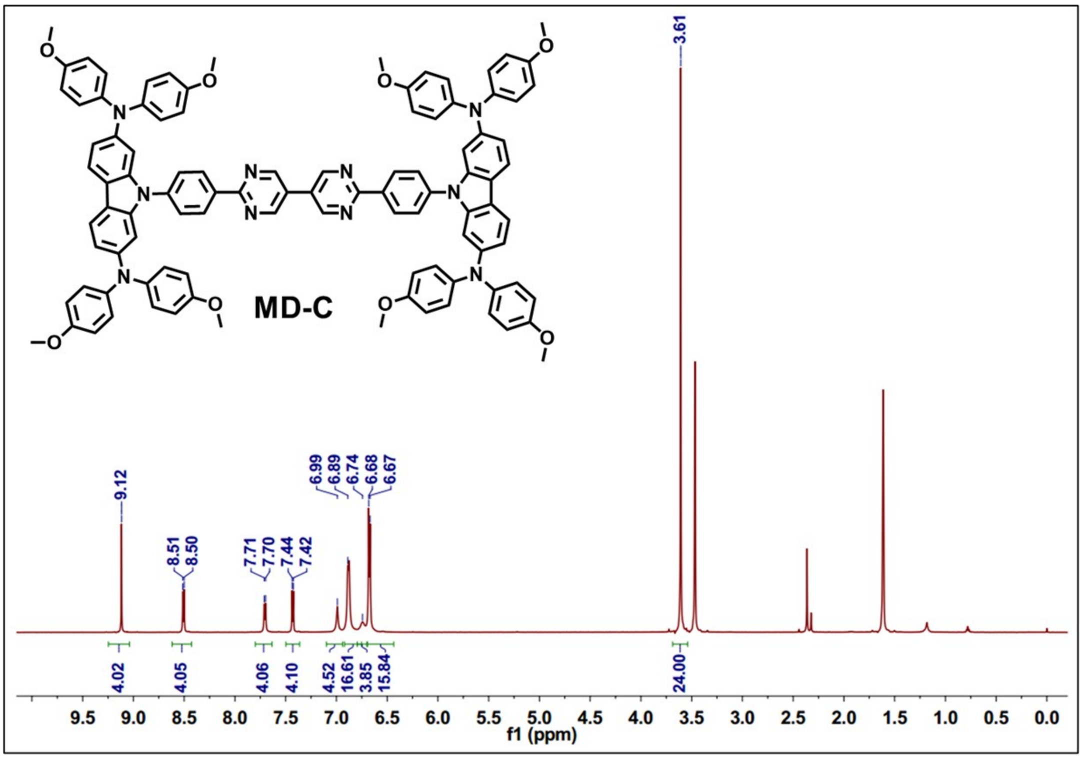

Figure S3. ^{1}H NMR spectrum of **MD-C** in THF - *d*^{8}

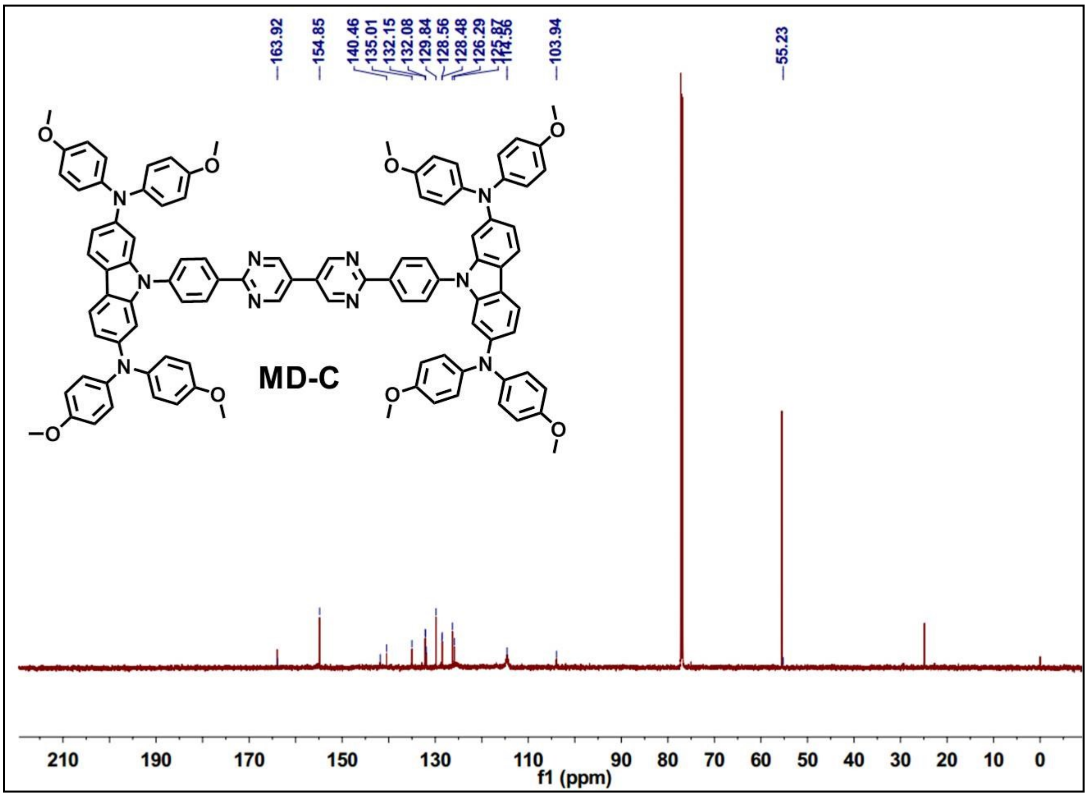

Figure S4. ^{13}C NMR spectrum of **MD-C** in $CDCl_3$.

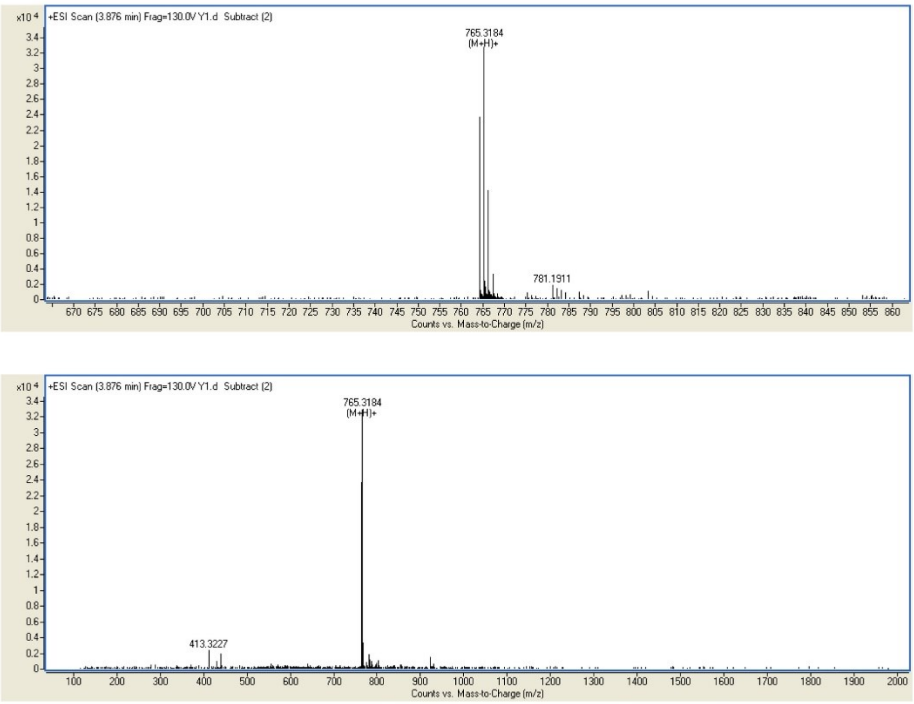

Figure S5. High resolution mass spectrometry of **MD-T**

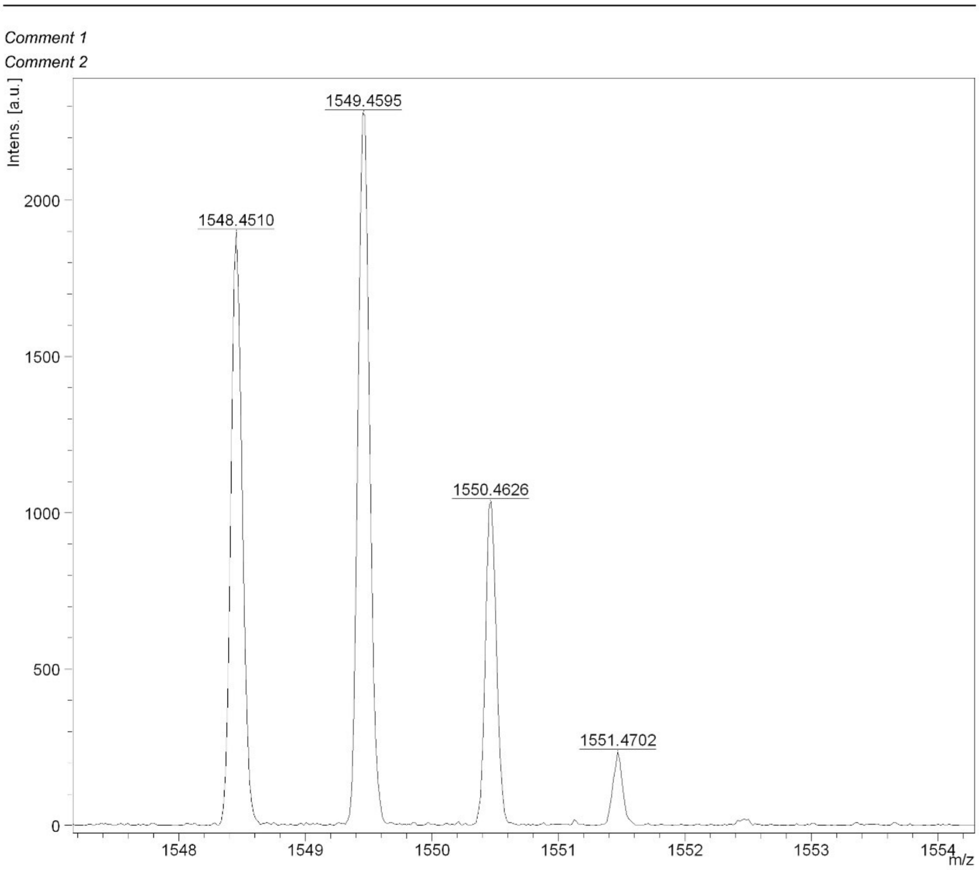

Figure S6. MALDI-TOF mass spectrometry of **MD-C.**

3. Cyclic voltammetry measurements

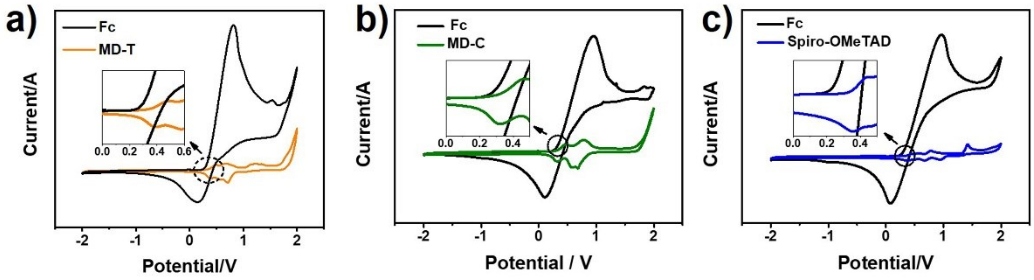

Figure S7. CV curves of MD-T and MD-C together with Spiro-OMeTAD

4. Thermal properties

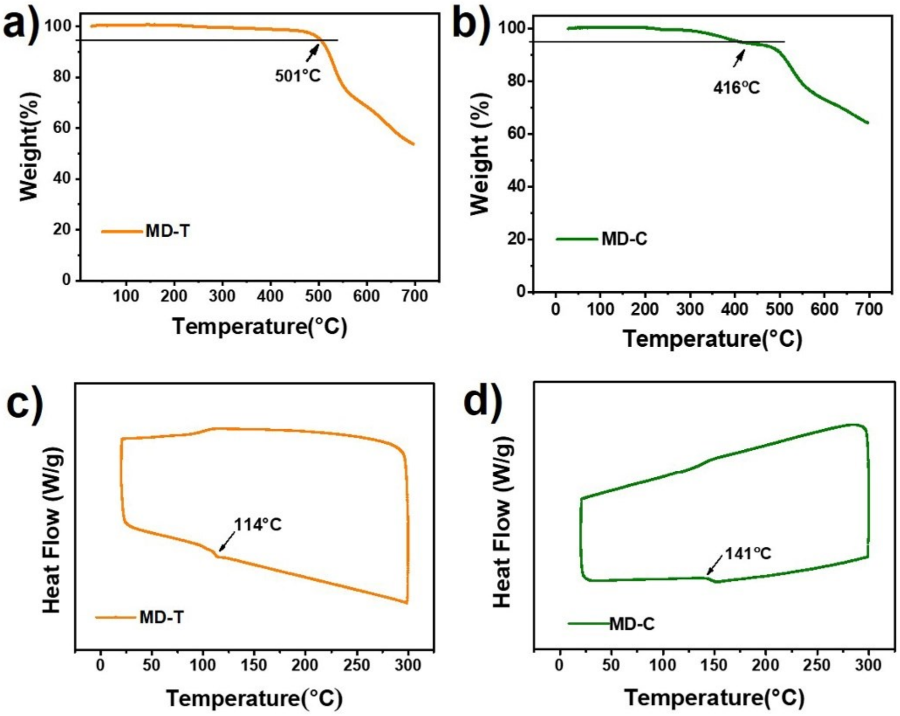

Figure S8. a), b) Thermogravimetric analysis (TGA) and c), d) Differential scanning calorimetry (DSC) of MD-T and MD-C under N_2 atmosphere.

5. Device materials, fabrication and testing

Materials

In this work, all major materials were purchased from commercial suppliers and used without further purification, including PEDOT:PSS (Heraeus, Clevios PVP Al 4083), PbI_2 (*p*-OLED, >99.99 %), $PbCl_2$ (*p*-OLED, >99.99 %), MAI (*p*-OLED, ≥99.5 %), C_{60} (*p*-OLED, >99.5 %), Spiro-OMeTAD (*p*-OLED, ≥99.5 %), MoO_3 (Sigma-Aldrich, 99.97 %), DMF (Sigma-Aldrich, 99.8 %), DMSO (Sigma-Aldrich, 99.8 %), THF (J&K, 99.9%) and CB (Sigma-Aldrich, 99.8 %).

Device fabrication and testing

Preparation of HTM Solutions

As for the reference, the Spiro-OMeTAD solution was prepared according to the literature. To prepare the solution, 72.5 mg Sprio-OMeTAD was dissolved 1 mL chlorobenzene with 28.5 μL 4-tertbutylpyridine (*t*BP) and 17.5 μL lithium-bis(trifluoromethanesulfonyl)imide (Li-TFSI) stock solution (520 mg mL^{-1} in acetonitrile) as additives. Different HTMs (MD-T and MD-C) were all dissolved in chlorobenzene with a concentration of 50 mg mL^{-1}, with *t*BP and Li-TFSI as dopants.

Device fabrication

All major device fabrication procedures were similar to those reported structure (FTO/compact TiO_2/Perovskite/HTM/Ag electrode). FTO-coated glass with sheet resistance of 14 Ω sq^{-1} was washed by sonication with deionized water, ethanol and acetone and then treated with oxygen plasma for two minutes. A compact layer of TiO_2 was deposited on the FTO substrate by spin-coating the titanium precursor (350 μL titanium isopropoxide and 25 μL HCl in 5 mL isopropanol) at 5000 rpm for 60 s following by calcination on a hotplate at 500 ^{o}C for 60 min (275 °C for 5 min, 325 °C for 5 min, 375 °C for 5 min, and 500 °C for 60 min). Afterward, mixed-lead-halide perovskite precursor (The mole ratio of PbI_2:$PbCl_2$:MAI is 1:1:4, 202.8 mg PbI_2, 122.7 mg $PbCl_2$ and 279.8 mg MAI in 1 mL DMF) was spin-coated on the substrate in sequence at 2000 rpm for 60 s. The substrates were then annealed under dark (usually at 95 °C) for 40 mins in a nitrogen filled glove box. After cooling down, hole transporting layer (HTL) was deposited onto the perovskite flm by spin coating at 5000 rpm for 60 s and oxidized in air for 15 h. Finally, Ag counter electrode (100 nm) was deposited by thermal evaporation.

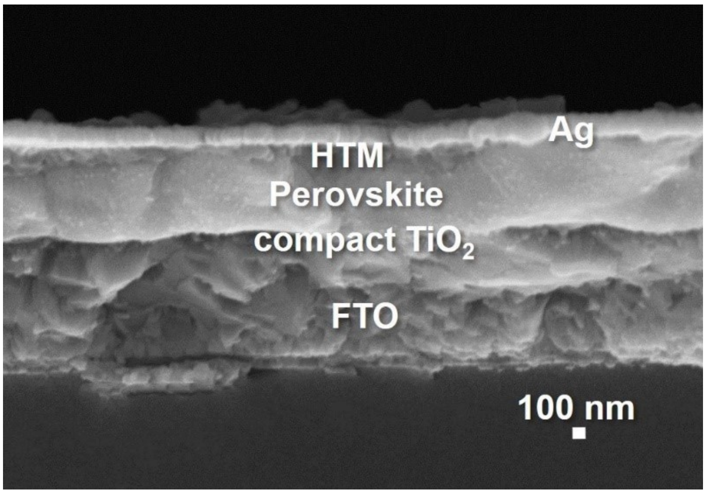

Figure S9. Cross-sectional SEM image of PSCs with the device structure of FTO/compact TiO_2/Perovskite/HTM/Ag electrode

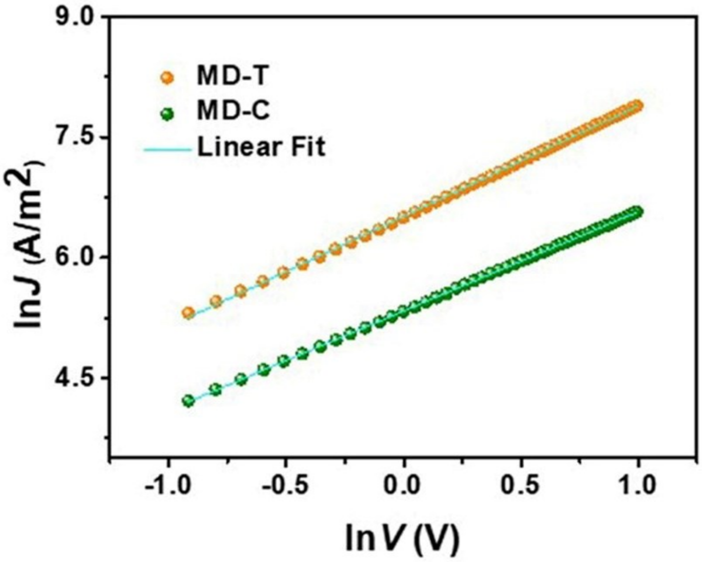

Figure S10. Measured hole mobility of the MD-T and MD-C with the SCLC method

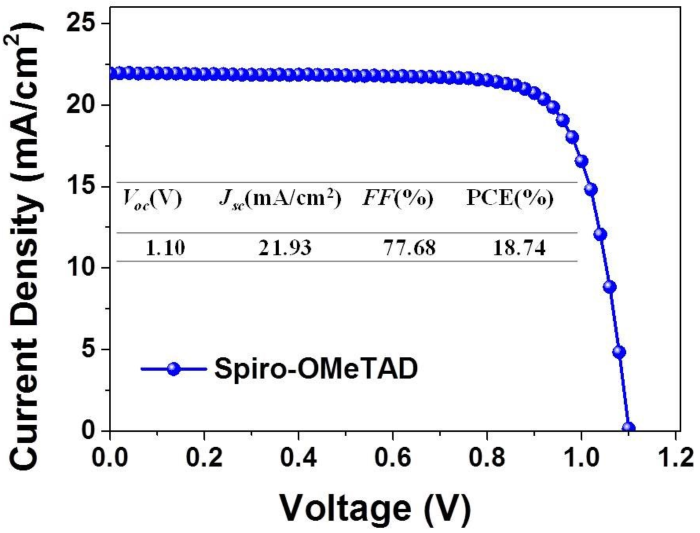

V_{oc}(V)	J_{sc}(mA/cm^2)	*FF*(%)	PCE(%)
1.10	21.93	77.68	18.74

Figure S11. *J–V* characteristics of the PSCs devices based on Spiro-OMeTAD

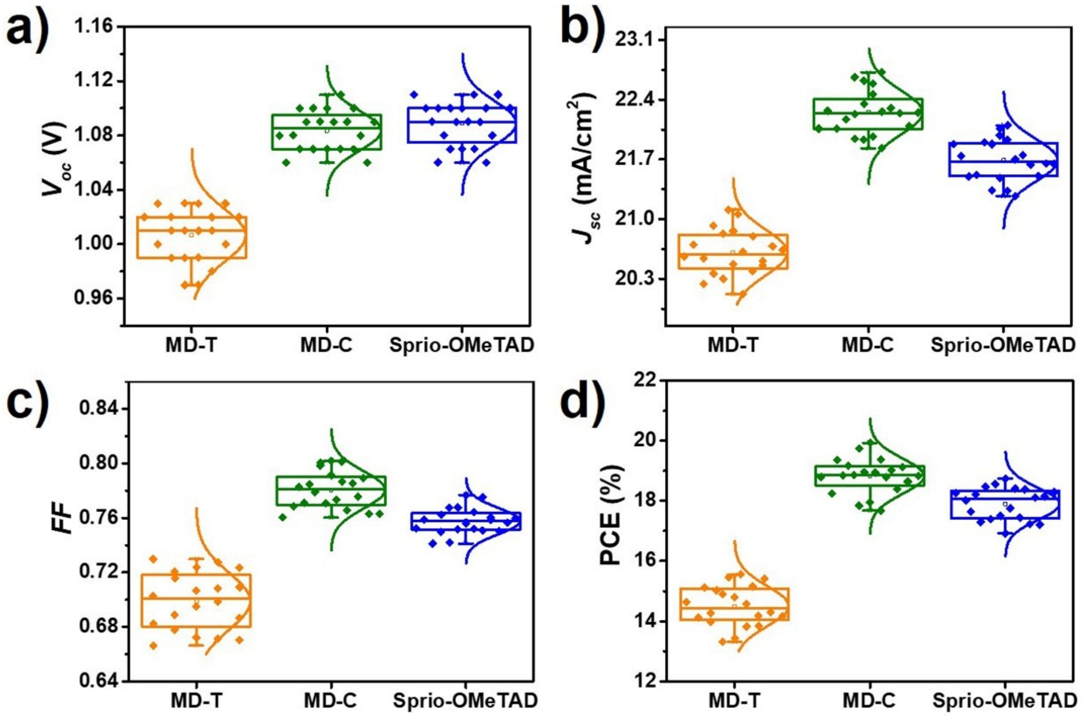

Figure S12. Box charts of (a) V_{oc}, (b) J_{sc}, (c) *FF*, and (d) PCE measured using reverse scans for 20 devices based on the MD-T and MD-C

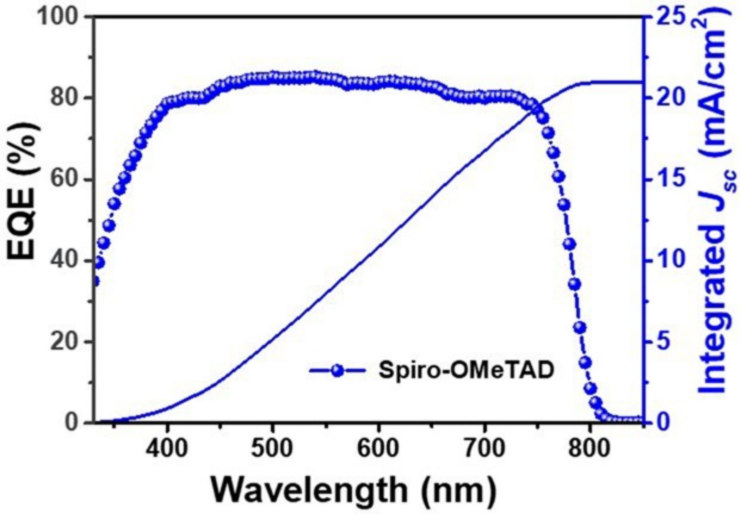

Figure S13. IPCE plots and integrated current densities of perovskite solar cells based on the Spiro-OMeTAD

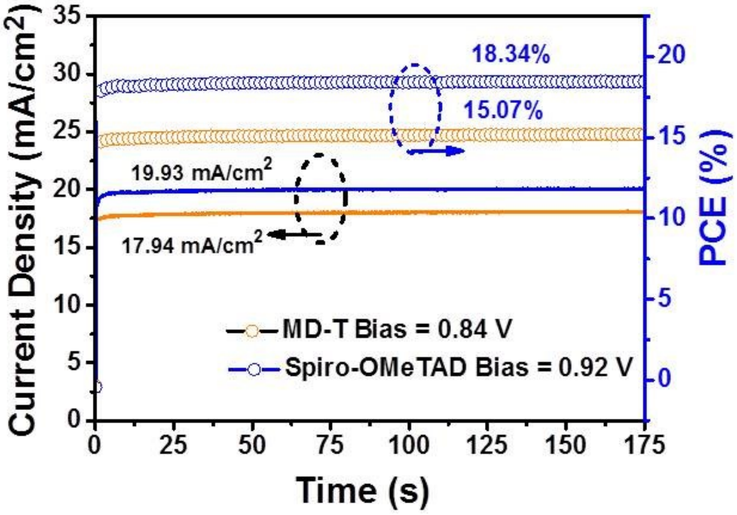

Figure S14. Stabilized power output of PSC devices for MD-T and Spiro-OMeTAD at their maximum power point

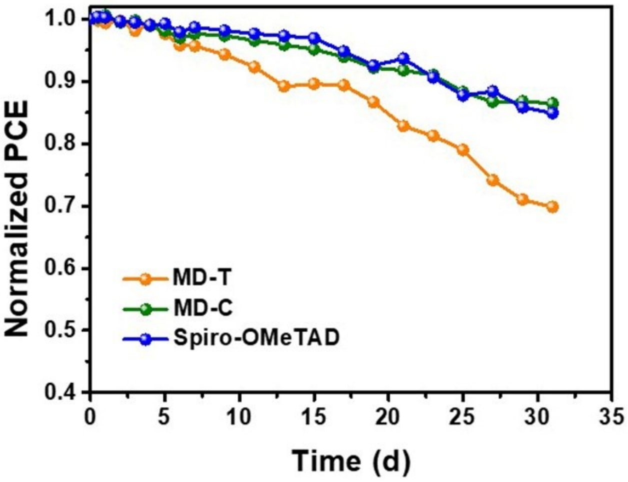

Figure S15 Stability test of MD-T, MD-C and Spiro-OMeTAD based PSCs (unencapsulated) in N_2 atmosphere over 30 days

Table S1. Photovoltaic parameters of perovskite solar cells using MD-T and MD-C as HTMs measured from forward scanning and reverse scanning

HTM	Scan Direction	V_{oc}(V)	J_{sc}(mA/cm^2)	*FF*	PCE (%)
MD-T	forward	1.03	20.94	0.72	15.55
	reverse	0.99	21.87	0.66	13.76
MD-C	forward	1.10	22.57	0.80	19.93
	reverse	1.08	22.63	0.77	19.02

Reference

1. H.-J. Park, S. H. Han, J. Y. Lee, H. Han and E.-G. Kim, *Chemistry of Materials*, 2018, **30**, 3215-3222.
2. Y. Ji, B. He, H. Lu, J. Xu, R. Wang, Y. Jin, C. Zhong, Y. Shan, F. Wu and L. Zhu, *ChemSusChem*, 2019, **12**, 1374-1380.